https://doi.org/10.48048/tis.2022.4977

Overtopping Scour due to Tsunami Bore: Laboratory Study

Raidan Maqtan[1,2,*], Badronnisa Yusuf[1] and Saiful Bahri Hamzah[3]

[1]Department of Civil Engineering, University Putra Malaysia, Selangor, Malaysia
[2]Department of Civil Engineering, University of Aden, Aden, Yemen
[3]National Hydraulic Research Institute of Malaysia, Selangor, Malaysia

([*]Corresponding author's e-mail: ridan76@yahoo.com)

Received: 6 December 2020, Revised: 11 September 2021, Accepted: 18 September 2021

Abstract

Tsunami wave is one of the most serious threats to lives and activities, particularly in coastal cities within 100 m height from the mean sea level. Construction of coastal defense structures, such as seawalls and breakwaters, is the most popular measure adopted by engineers for protection from sea waves, including tsunamis, and mitigation of their effects. Many researchers determined through their post-tsunamis field studies that the scour at the landward toe of coastal defense structures induced by tsunami overtopping is the predominant cause of structural failures. İn the present study, a series of laboratory experiments was conducted at National Hydraulic Research Institute of Malaysia to investigate the scour profile at the landward toe of a vertical seawall induced by tsunami bore overtopping vertical seawall and examine the influence of breakwater and bore characteristics on the induced scour depth and length. The experiments showed that the breakwater in low initial depth conditions was more effective in reducing bore velocity and scour depth at the landward toe of the seawall than that in high initial depth conditions. Moreover, a strong positive relationship was confirmed between the Froude number of the overtopping flow and the induced scour depth and length.

Keywords: Tsunami, Overtopping, Seawall, Scour, Breakwater

Introduction

The word *tsunami* came from Japan, where "tsu" means harbor, and "name" means wave. A violent earthquake underwater usually generates tsunamis, but they may also be triggered by other events, such as the impact of meteor and landslide undersea [1]. Through the past 20 years, massive earthquakes followed by tsunamis, such as the tsunami of Indian Ocean in 2004, the 2010 tsunami of Chile, and the 2011 tsunami of Tohoku, have caused considerable loss of lives and damage to nature [2].

Environment of the coasts provides desirable sources of live standards which encourage peoples to stay in dense population close to coastline. These coastal zones of high population density which lie within 100 km close to shore line and on range of 100 m high from the mean sea level can reach 2.5 times more in population than that exist in other villages near the coast [3]. For this reason, the vulnerability of these communities to coastal hazards such as hurricanes and tsunamis is more, and this is one of the important reasons which hearten engineers and researchers to be more aware about the protection and mitigation processes. The coastal defense measures can be classified into 2 categories, direct and indirect measures [4]. Construction of seawall parallel to the shore line is one of the direct measures used to protect from flooding.

As an effective method of beach protection, seawall construction was adopted for regions where excessive beach erosion causes further damages. For instance, seawalls (vertical in many cases) are built to create a boundary line separating land and seawater when seawater is about to extend over buildings or roads [5]. Since the 1960 Chilean tsunami, the Japanese have used seawalls and armored dikes parallel to the shoreline. Data history of tsunamis and storm surges is generally used to determine the required height of seawalls and coastal dikes [6].

Tsunamis that ultimately reach the beaches may generate a series of turbulent bores flowing directly to shallow water or may collapse on coastal defense structures generating an overtopping flow. These devastating waves can produce different structural failure mechanisms, including large-scale scouring and sedimentation around the coastal structures [7]. Many post-tsunami field surveys conducted by

researchers and engineers [6], [8-10] indicated that the scour at the landward toe of the seawalls or coastal dikes induced by tsunami overtopping is the predominant cause of structural failure.

This study is an extension of a previous laboratory study [11] conducted to investigate the effects of different flow parameters associated with tsunami bore on the scour profile at the landward toe of a vertical seawall. In the present study, the breakwater was installed in the model, and the experiments were conducted in the same previous physical model with the same flow conditions to observe the influences of the breakwater. The bore-like tsunamis were generated using dam break technique in 100 m-long flume and allowed to impinge and overtop the breakwater and then the seawall on a beach slope of 1:10. The incident, overtopping bore characteristics, and the scour profile at landward toe of the seawall were investigated before and after installing the breakwater model.

Background

The common techniques usually applied to determine and understand the local situations caused by cyclones or tsunami waves include physical modeling, numerical modeling, and field survey after the disaster. Shimozono and Sato [12] conducted extensive post-tsunami field surveys after the 2011 Tohoku tsunami in Japan. Their study focused on the failure of concrete armored levees by local landward scouring that was widely observed. They observed that the main cause of downstream breaching of the concrete armored levees is the excessive scouring at the landward toe. The dominant cause of coastal dike failure in the 2011 tsunami at the coasts of Iwate, Miyagi, and Fukushima Prefectures is the excessive scouring near the landward toe of the structures [6,8,13].

Tappin *et al.* [14] applied different techniques, including post-tsunami field observations, satellite images, and videos, to investigate the tsunami impacts on the eastern Japan coastal zones and compared the coasts with and without structural protections. They observed a severe scouring at the landside toe of high concrete embankments at the hardly protected coasts. The impacts of coastal defense structures and coastal forest and vegetation on mitigating tsunamis were investigated using field data and numerical simulations [9,15]. The liquefaction associated with earthquakes, which decreases the effective stress, was reported and investigated experimentally by [16]. They found that this phenomenon affects the scour profile generated downstream of the seawall because of tsunami overtopping. El-bisy [17] investigated the bed changes and influence of different parameters, including grain size of bed material, steepness of wave, and position of seawall, on the scour phenomenon at the landward toe of the seawalls. Robertson *et al*. [18] conducted laboratory experiments using the concept of solitary wave-like tsunami to investigate the forces induced by tsunami bores on vertical seawalls. Jayaratne *et al*. [8] investigated the scour profile downstream of coastal dike model generated by tsunami overtopping by applying dam break technique. They observed that a strong relationship exists between downstream slope angle of the dike and the maximum scour depth.

Predictive models

Tsunami overtopping discharge and scour induced by tsunamis are very complicated processes because many parameters are involved. The studies that produced predictive models to calculate the overtopping discharge and/or scour depth induced by tsunamis at the landward toe of seawalls are very limited.

Scour depth

Jayaratne *et al*. [13] developed a representative scour depth model for coastal dikes based on the field survey data of the 2011 Tohoku Tsunami. Jayaratne *et al*. [8] conducted a series of laboratory experiments to analyze and refine the model. The developed model is presented in Eq. (1);

$$\frac{D_s}{H_{d2}} = \lambda\left(exp - \left(\frac{\sqrt{H_{d2}}}{2\lambda\sqrt{h}\,\sin\theta_2}\right)^4\right) \qquad \begin{cases} h > 0 \\ 10^4 < k < 10^3 \end{cases} \tag{1}$$

where D_s is relative scour depth, H_{d2} is the height of the coastal structure measured from the leeward toe, h is inundation height, θ_2 is the angle of leeward slope, λ is scour coefficient (= 0.85), and k is Darcy's coefficient of permeability (m/s).

The scours at the landward toe of coastal structures induced by the tsunamis in 2004 and 2011 were measured and evaluated for many tsunami-affected cities [10,19]. Eq. (2), used for plunging scour and developed by [20], was applied to evaluate and compare the measured results [10].

$$D_s = C_{2v}\sqrt{q\ U\ \sin\theta/g} \quad (2)$$

where D_s is scour depth, C_{2v} is coefficient of scour taken as 2.8, and discharge per unit width q can be calculated using the standard discharge equations for wide-crested weir [10], U is approaching jet velocity $=\sqrt{2\ g\ H_o}$, and θ is the angle between the horizontal and the jet.

Wave overtopping discharge

Tsunamis, storm surges, and other extreme waves may cause overtopping flow over the coastal defense structures, such as seawalls, breakwaters, and dikes. Overtopping discharge is one of the critical parameters required for coastal defense structures design. Many predictive formulas have been developed and/or discussed by researchers [21-27] to predict wave overtopping discharges. However, most of these predictive models are restricted with limited boundary conditions regarding breaking, offshore conditions, and limited values of freeboard. One of the complicated conditions still under question is a long wave that occurs because of wave breaking caused by very shallow foreshore conditions [28], and the other case is overtopping at low and zero freeboard conditions [22].

A numerical model [29] was applied to estimate the wave overtopping discharge. The model was compared with Eq. (3) expressed by Chadwick *et al.* [30], which was used to calculate the overtopping discharge over broad-crested weir;

$$q = 1.705 C_d H_o^{\frac{3}{2}} \quad (3)$$

where q is the discharge over weir, H_o is overflow height, and C_d is discharge coefficient, presented as;

$C_d = 0.848 C_f$, and $C_f = 0.91 + 0.21\frac{H_o}{B_l} + 0.24\left(\frac{H_o}{H_o+H_B} - 0.35\right)$

where H_B is weir height, and B_l is weir width.

The exponential Eq. (4) is widely used to predict the wave overtopping discharge for many types of seawalls;

$$\frac{q}{\sqrt{g\ H_{m0}^3}} = a\ exp\left[-b\ \frac{R_c}{H_{m0}}\right] \quad (4)$$

where q is discharge per length, H_{m0} is spectral significant wave height, R_c is freeboard, and a and b are fitting coefficients. The left-hand side of Eq. (4) is called dimensionless overtopping discharge. In case of nonbreaking wave overtopping vertical seawall, simple values, such as a = 0.2 and b = 4.3, can be used for the fitting coefficients for relatively deep water; alternatively, a = 0.05 and b = 2.78 can be used for the fitting coefficients for shallow water [22].

Materials and methods

Model scaling

The physical models in hydraulic laboratories are small representations of real-world hydraulic problems (prototypes). A suitable scale factor can be calculated by dividing the length of the prototype over the model length, see Eq. (5). The scale factor should be kept as small as possible to minimize the effects of scale. Scaling the conditions of a prototype to a physical model in the laboratory is challenging. Geometric similarity can be achieved by keeping the shape the same as that of the prototype with dimensions smaller than those of the physical model. Froude scaling is usually adopted to scale the gravity-free surface flow as illustrated by Eq. (6), where v and d are the velocity and height of the incoming jump, respectively [31]. Accordingly, the bore characteristics can be scaled by using Eq. (7) for velocity and Eq. (8) for time. The scale of the model for this study is taken as $L_r = 20$. The symbols T and v represent time and velocity, and the letters m and p refer to model and prototype scales, respectively.

$$L_r = \frac{L_p}{L_m} \quad (5)$$

$$F_r = \frac{v}{\sqrt{gd}} \quad (6)$$

$$F_r = \frac{v}{\sqrt{gd}} \quad (7)$$

$$T_p = T_m\sqrt{L_r} \quad (8)$$

Experimental setup and instrumentation

The lab experiments were conducted at National Hydraulic Research Institute of Malaysia (NAHRIM) in a 100 m-long flume with width and height of 1.5 and 2.0 m, respectively. An electrically controlled steel gate was installed at 45 m from the back end of the flume. The part of the flume upstream of the gate was utilized as a water tank storing water to the required level. The other part of the flume length downstream of the gate was utilized for constructing the designed model, as shown in **Figure 2**. One of the flume side walls provided with a glass wall supported by steel columns is shown in **Figure 1**. All the experiments were conducted with and without breakwater to allow the effects of the breakwater on bore characteristics and landward scour. A porous type breakwater with a height of 20 cm (4 m height in prototype scale) was fixed on the flume bed at a distance of 5 m (100 m in prototype scale) upstream of the seawall, as shown in **Figure 2**.

Six wave gauges were installed at selected locations to measure the water surface elevations, as shown in **Figure 2**. The wave gauges were numbered from WP1 until WP6, where the name WP1 represents wave probe number 1. Readers can refer to [11] for other details about instrumentation. In the beginning, the experiments were conducted for high, medium, and low relative depth conditions without breakwater with 3 times repetition for each case. Then, the porous breakwater was fixed in the position, **Figure 3**. Then, the experiments were repeated with breakwater for the 3 min cases with the same previous hydraulic conditions. A typical scour profile photo is shown in **Figure 4**.

Figure 1 Wave flume at NAHRIM.

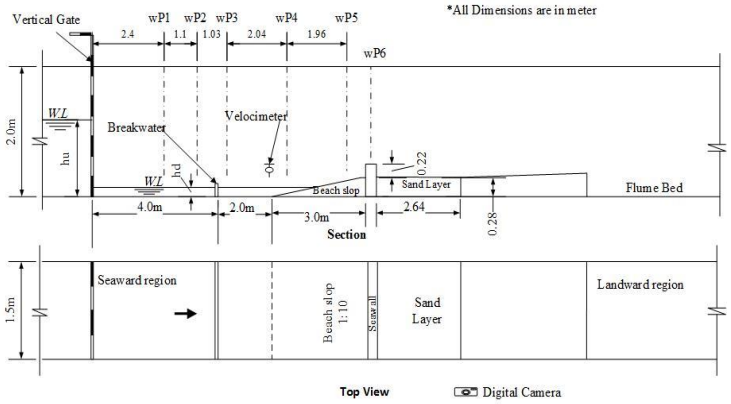

Figure 2 Experimental setup schematic drawing.

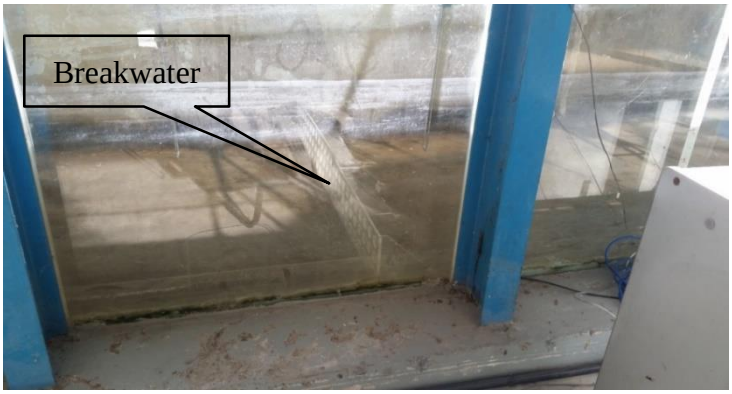

Figure 3 Photograph of the breakwater fixed on the flume.

Figure 4 Typical scour profile photograph [11].

Experimental details

The experiments were numbered from T1 to T6 with detailed conditions for all tests arranged, as shown in **Table 1**. The symbols h_u and h_d explained in **Figure 2** and in **Table 1** represent the water levels of the upstream and downstream of the gate, respectively, immediately before the gate was opened to generate bore-like tsunami.

Table 1 Tests details and conditions (values in model scale).

Test	h_u (m)	h_d (m)	Conditions
T1	0.6	0.1	without breakwater/ low relative depth
T2	0.9	0.15	without breakwater/ medium relative depth
T3	1.2	0.2	without breakwater/ high relative depth
T4	0.6	0.1	with breakwater/ low relative depth
T5	0.9	0.15	with breakwater/ medium relative depth
T6	1.2	0.2	with breakwater/ high relative depth

Results and discussion

The experiments were conducted by following the same arrangement, as shown in **Table 1**. Some difficulties were encountered in taking the measurements and observations because the run time of each experiment was very short. In addition, the scour measurements after each run could not be taken unless the water drained totally from the sand layer, which takes a long time. However, all the required measurements and observations were taken, and the results and discussion for each parameter effect were presented separately in the following sections.

Breakwater effects on the scour profile and tsunami bore characteristics

The experiments T1 and T4 were assumed to represent the low relative depth condition without and with breakwater, respectively. The reason is that the lowest value of the initial water level in these tests was fixed at the front of the seawall and beach slope during testing. The water level upstream of the gate was fixed at 0.6 m from the flume bed level, and the water level downstream of the gate was fixed at 0.1 m from the bed. Then, the gate was opened electrically for 10 s, and the water was allowed to free fast flow because of the head difference upstream and downstream of the gate. The maximum bore velocities for the low relative depth condition without and with breakwater were determined as 1.585 m/s (7.1 m/s in prototype scale) and 1.427 m/s (6.4 m/s in prototype scale), respectively. The results of velocities for this situation indicated that the velocity for test condition T4 (with breakwater) was less than that for test condition T1 (without breakwater). The reduction in the bore velocity due to the existence of the breakwater was approximately 10 %. The maximum bore height for these flow conditions was 3.8 m (in prototype scale), occurring on the beach slope (without breakwater). The maximum bore height for this case recorded by WP5 was 3.6 m on the prototype scale, occurring on the beach slope. The maximum overtopping water thickness observed from the video was 0.05 cm (1.0 m on the prototype scale). Therefore, the reduction of the bore height due to the introduction of the breakwater was 0.2 m or 5.3 % of the height without breakwater. The maximum scour depth obtained without breakwater in T1 test was 5.8 cm (1.16 m in prototype scale), and that with breakwater in T4 test was 4.6 cm (0.92 m in prototype scale). The maximum scour lengths from the landward face of the seawall for the 2 cases were nearly the same, that is, 40 cm or 8 m in prototype scale.

The tests T2 and T5 represent the medium relative depth conditions without and with breakwater, respectively. The water level upstream of the gate was fixed at 0.9 m from the flume bed level, and the water level downstream of the gate was fixed at 0.15 m from the bed level of the flume. The run time and other testing procedures were the same as those explained in low relative depth conditions. The maximum bore velocities from these flow conditions were 1.807 m/s (8.1 m/s in prototype scale) and 1.793 m/s (8.02 m/s in prototype scale) for tests T2 and T5, respectively. The reduction in the bore velocity due to the introduction of breakwater in these flow conditions was approximately 1 % only. The maximum height of the incident bore generated for these flow conditions was 0.43 m (8.6 m in prototype scale) without breakwater and 0.33 m (6.6 m in prototype scale) with breakwater. The maximum scour depths generated in this case without and with breakwater were 11.7 cm (2.34 m in prototype scale) and 11.1 cm (2.22 m in prototype scale), respectively. From the other side, the scour length generated in the case of no breakwater was 120 cm (24 m in prototype scale), whereas that generated with breakwater was 110 cm (22 m in prototype scale) from the landward face of the seawall.

The tests T3 and T6 represent high relative depth conditions without and with breakwater, respectively. The water level upstream of the gate was fixed at 1.2 m from the flume bed level, and the water level downstream of the gate was fixed at 0.2 m from the bed level of the flume. The run time and other testing procedures were the same as those explained in low and medium relative depth conditions. The maximum bore velocities from these flow conditions were 2.08 m/s (9.3 m/s in prototype scale) and 2.06 m/s (9.21 m/s in prototype scale) for tests T3 and T6, respectively. The reduction in the bore velocity due to the introduction of the breakwater in these flow conditions was also approximately 1 % only. The maximum height of the incident bore generated for these flow conditions was 0.59 m (11.8 m in prototype scale) without breakwater and 0.46 m (9.2 m in prototype scale) with breakwater. The maximum scour depths generated in this case without and with breakwater were 11.9 cm (2.38 m in prototype scale) and 11.5 cm (2.3 m in prototype scale), respectively. From the other side, the scour length generated in the case of no breakwater was 185 cm (37 m in prototype scale), which was more than that generated with breakwater at 160 cm (32 m in prototype scale) from the landward face of the seawall.

Overtopping velocity

The maximum flow velocities of the water overtopping seawall were measured using a current meter fixed in an appropriate position at the top of the seawall model. The incident bore velocities for different tests conditions are discussed in the preceding section, and the overtopping velocities recorded for all tests conditions are summarized in **Table 2**. The experiments showed that the incident velocities ranged from 6.4 to 9.3 m/s, and the overtopping velocities ranged from 0.22 to 5.68 m/s. These experimental values were comparable with the tsunami velocities reported in some locations by field survey [32] and video analysis [33] during the Indian Ocean Tsunami 2004 [34].

Initial relative depth (relative freeboard)

The results showed that the initial water depth h_d upstream of the seawall greatly affects the induced scour profile downstream of the wall. High initial upstream depth (low freeboard height, R_c) produced high scour depth D_s and length L_s at the landward toe of the seawall, and vice versa. The same effect with different values was observed in the case of with or without the breakwater model. In general, the flow resistance to the incoming bore is low because of the effect caused by high initial water depth. Accordingly, this scenario results in a high overtopping discharge and high scour depth and length. The non-dimensional relation is presented graphically in **Figure 6**. In these graphs, the term *relative freeboard* R_c/h_w is used instead of *relative depth* because the former is commonly used in similar studies. The graphs showed negative trend relations of the correlation factors 0.77 and 0.97 with scour depth and length, respectively. R_c is the elevation difference between seaward initial water level and crest level of the seawall, and h_w is the clear height of the seawall.

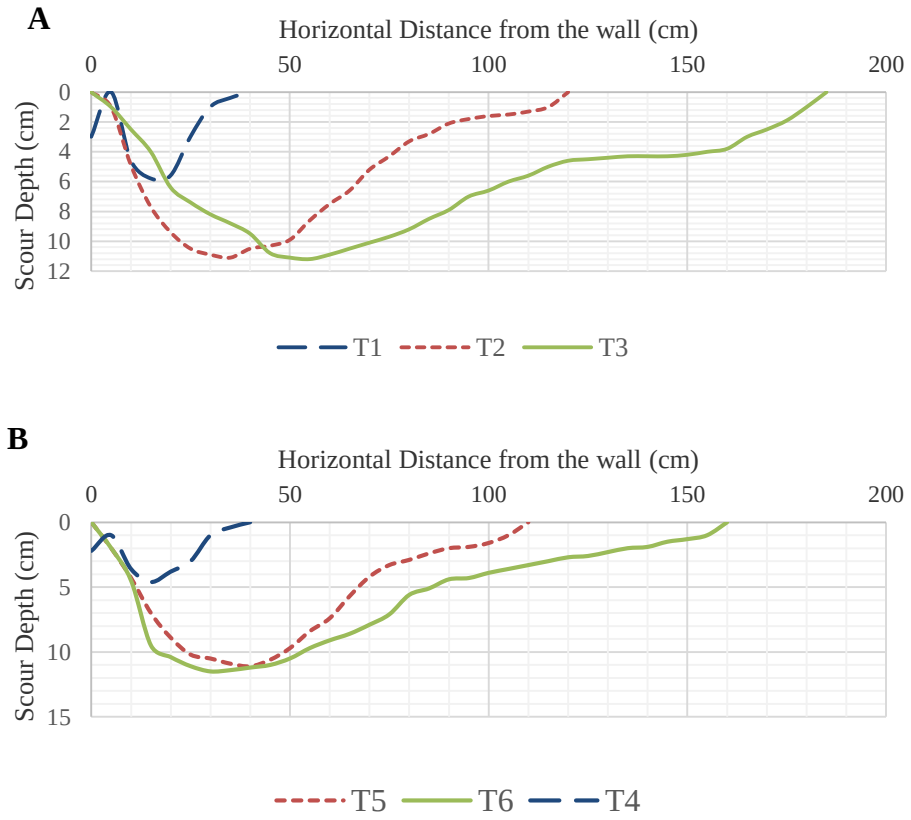

Figure 5 Scour profiles generated at the landward toe of the seawall (A) Without breakwater [11]; (B) with breakwater.

Table 2 Overtopping velocities summary.

Test conditions	Overtopping velocity, v_o (prototype) m/s
T1	0.22
T2	3.98
T3	5.68
T4	0.13
T5	3.71
T6	5.41

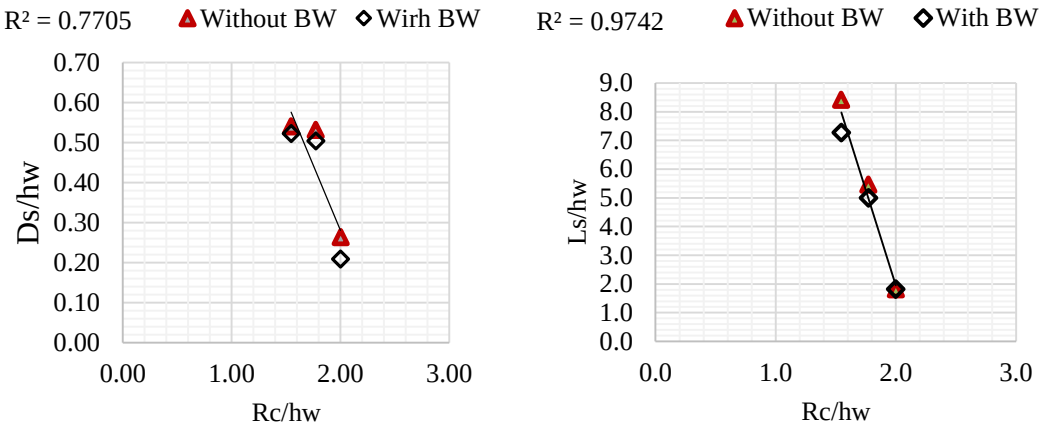

Figure 6 Non-dimensional relationship between the seaward initial water level and the maximum scour depth and length generated.

Bore height

Incident bore

Tsunami bore reaches its maximum height when it approaches shallow water near the coastline. In this study, the term incident bore height represents the maximum height of the generated bore before striking the seawall model. The experiments showed that direct proportion relations exist between the incident bore height H_b and the induced scour depth and length. The graphs shown in **Figure 7** represent these relations. Moreover, the graphs indicated that strong positive relations exist between the parameters.

Overtopping bore

In general, the overflow water height (or sometimes water thickness) above the hydraulic structures is the most important parameter governing the discharge quantity. Thus, its effects on the scour depth and length landward of the seawall must be investigated. In this study, the overtopping flow height H_o refers to the maximum height of the overflowing water above the seawall model. The non-dimensional relationships between this parameter and the scour depth and length induced by landward toe are shown in **Figure 8**. The graphs indicated that strong positive relations exist between the parameters.

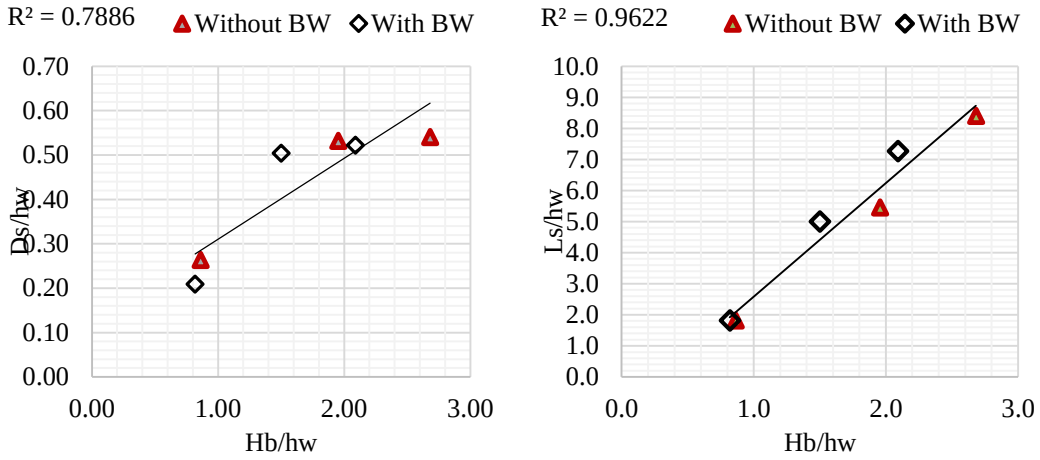

Figure 7 Non-dimensional relationships between the incident bore height and the maximum scour depth and length generated.

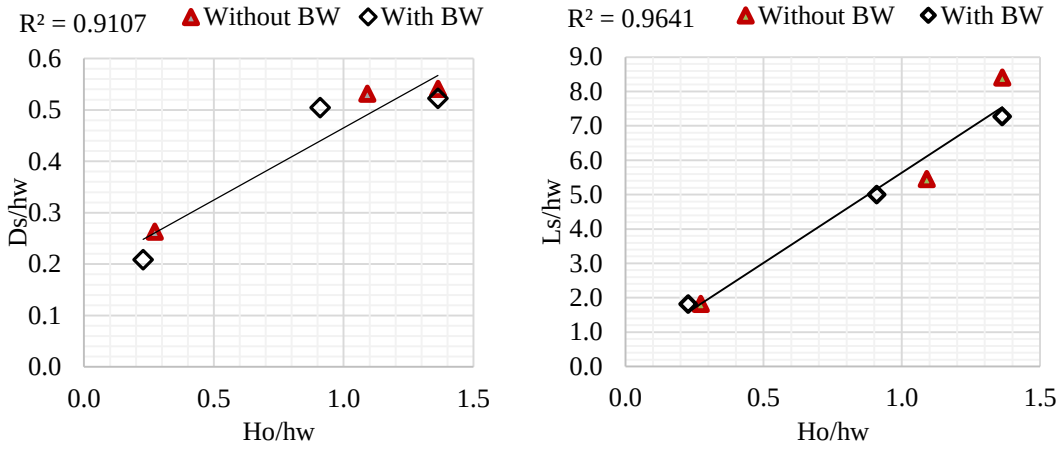

Figure 8 Non-dimensional relationship between the overtopping bore height and the maximum scour depth generated.

Froude Number

For incident bore

Froude number, an important parameter in hydraulics, determines the nature of the flow. Furthermore, it is commonly used for model scaling in open-surface flow. In this study, the incident Froude number F_b for the incoming flow defined in terms of the incoming velocity v_b, height of the incoming bore H_b, and gravitational acceleration g is described in Eq. (9).

$$F_b = \frac{v_b}{\sqrt{gH_b}} \tag{9}$$

The non-dimensional relationship between the Froude number of the incoming flow and the maximum scour depths and lengths is shown in **Figure 9**. The graphs showed a negative trend in both cases with correlation factors 0.75 and 0.79 for relative scour depth and length, respectively. This negative trend is related to the calculated values of Froude number according to these experimental conditions. This trend may also be related to the flow states associated with different values of Froude number. For instance, if the Froude number is 1 or more, the flow is critical with high flow velocity and

relatively small flow depth. Thus, the scour downstream of the wall produced by the relatively fast flow with low depth upstream of the wall is lower than that produced by the flow with high depth upstream of the wall.

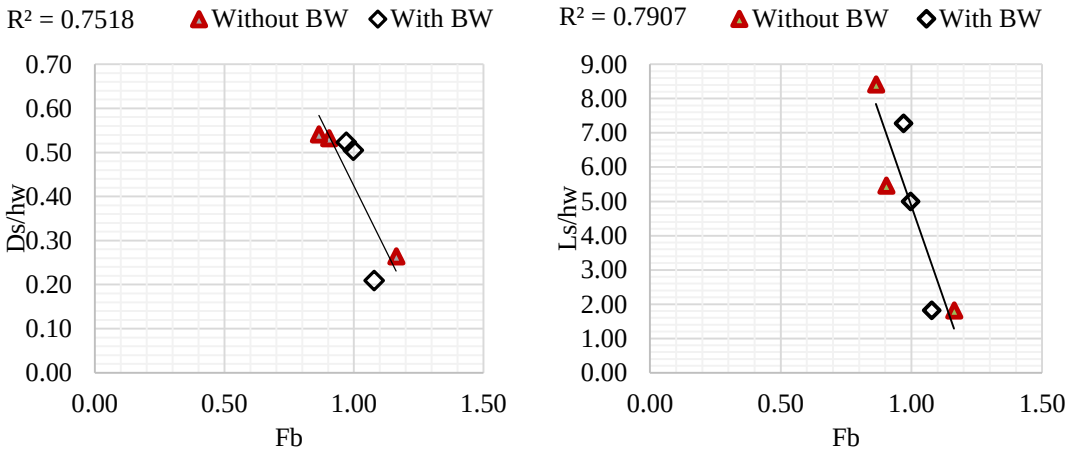

Figure 9 Non-dimensional relationships between the Froude number of the incident bore and the scour depth and length.

For Overtopping flow

In general, the overtopping flow characteristics directly affect the hydraulic environment downstream of the hydraulic structures. A large amount of the flow energy upstream of the seawall (seaward) is dissipated once the flow strikes the wall. Thus, the incident and overtopping Froude numbers have an important difference. In this study, the overtopping Froude number F_o is defined in terms of the maximum overtopping velocity v_o and the maximum flow height above the wall H_o, as described in Eq. (10);

$$F_o = \frac{v_o}{\sqrt{gH_o}} \tag{10}$$

The graphs in **Figure 10** indicated strong positive relations between the overtopping Froude number and the maximum induced scour depth and length. Furthermore, we observed by checking all the graphs that the strongest relations were determined with F_o and H_o, where the maximum values of R^2 have obtained. Thus, a simple predictive model (Eq. (11)) was proposed to consider the effects of both parameters F_o and H_o on the maximum induced scour depth. The model is entirely based on these experimental results.

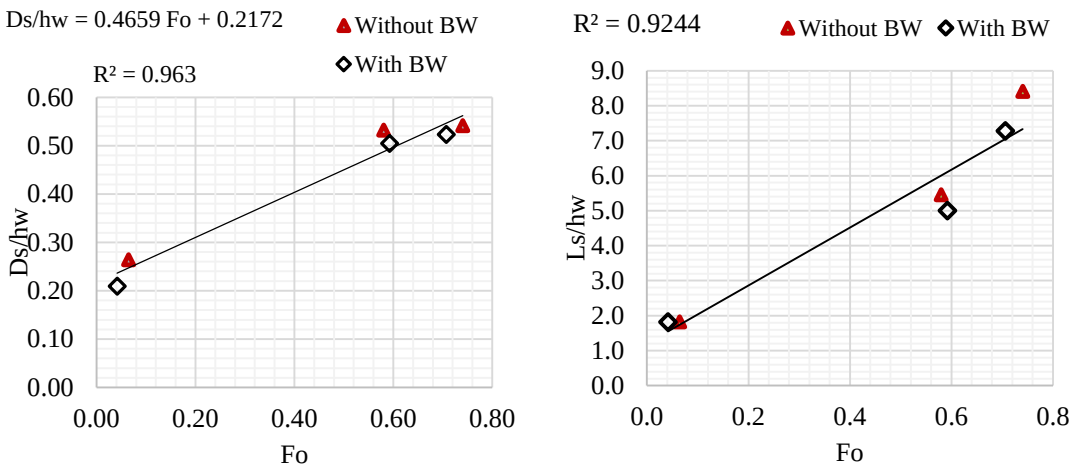

Figure 1 Non-dimensional relationship between the Froude number of the overtopping bore $F_o$and, the scour depth D_s and length L_s.

$$D_s = (0.466\ F_o\ + 0.217)\ h_w \quad (11)$$

Overtopping discharge

Most of the conducted studies about tsunami physical modeling have adopted solitary wave technique. Measuring the overtopping discharge of tsunami-like waves has not been covered well, particularly in studies that used dam break technique. In the present study, the overtopping discharge was not measured in the lab because of some difficulties, including a large amount of discharge in a very short time. However, the authors attempted to use some existing equations used to calculate the overtopping scour depth in terms of the overtopping discharge. Eq. (2) was applied in the calculations with 2 different ways of calculating the overtopping discharge q for comparison.

First, the overtopping discharge q was calculated using Eq. (3), which was used for the flow over the broad-crested weir. In this case, the flow in the model was assumed to behave as a broad-crested weir overflow with maximum water depth H_o above the crest. In addition, the coefficient of discharge C_d was calculated based on the model geometries described earlier. Second, the overtopping discharge was calculated by applying Eq. (4), which was widely used in calculating the overtopping discharge for ordinary waves. We have to assume a nonbreaking wave overtopping vertical seawall to make this equation applicable.

The results of calculations are presented graphically in **Figure 11** to compare the calculated and experimental values. The graph showed that the calculated scour depth values based on the wave overtopping discharge predicted by Eq. (4) are close to the experimental measurements.

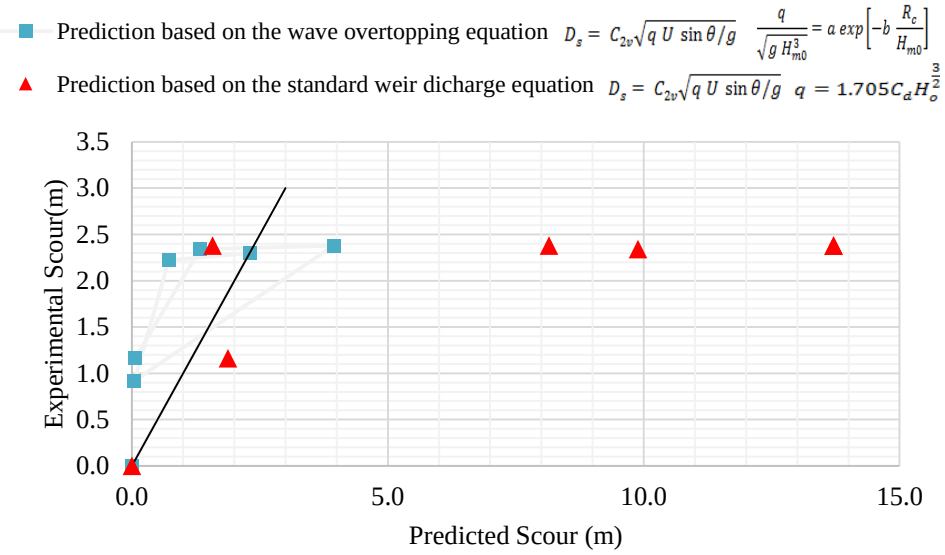

Figure 11 Measured and predicted maximum scour depth.

Conclusions

Tsunamis are the most devastating waves to the infrastructures in coastal cities, causing considerable loss in lives**.** Seawalls are one of the most commonly used measures for protection from sea waves, including tsunamis, and or mitigation of their effects**.** Providing full protection from tsunamis is a challenge or maybe impossible, depending on the devastating power of tsunamis. However, the construction of stable coastal defense structures against the worst conditions is essential in mitigating the risks of tsunamis**.** Most of the post-tsunami field surveys revealed that the scour at the landward toe of the seawall is the predominant cause of seawall failure after a tsunami**.** This laboratory study is intended to investigate the process, and the conclusions can be summarized in the following points:

1) The experiments were conducted to investigate the effects of a breakwater and some flow parameters on scour depth and length generated by tsunami at the landward toe of a vertical seawall. Three different cases of relative depth conditions with and without breakwater were adopted. The scour depth and length in low relative depth conditions are considerably smaller than those in the medium and high relative depth conditions. Furthermore, the comparison between medium and high conditions indicated that the scour depths are not considerably different, whereas the scour lengths are considerably different, as shown in **Figure 5**.

2) The effects of a breakwater on reducing bore velocity and scour profile in low relative depth conditions are higher than those in medium and high relative depth conditions. The reduction in bore velocity in low relative depth conditions is approximately 10 %, whereas that in medium and high relative depth conditions is approximately 1 %.

3) We determined by investigating the strength of the relation between the relative scour depth and the specified flow parameters that the strongest relation exists with the overtopping Froude number F_o.

Two different equations were used to calculate the overtopping discharge. One is the standard broad-crested weir discharge equation, and the other is the general exponential equation for wave overtopping. The results indicated that the calculated scour values based on the wave overtopping discharge approach are closer to the experimentally measured scour values than those based on standard broad-crested weir discharge equation.

Acknowledgements

The authors would like to thank the technical staff at National Hydraulic Research Institute of Malaysia for their help in conducting the experiments of this research.

References

[1] T Wang, T Meng and H Zhao. Tsunami loading analysis and engineering prevention and control. *Open Civ. Eng. J.* 2015; **9**, 376-81.

[2] H Park, DT Cox and AR Barbosa. Comparison of inundation depth and momentum flux based fragilities for probabilistic tsunami damage assessment and uncertainty analysis. *Coast. Eng.* 2017; **122**, 10-26.

[3] T Tomiczek, A Prasetyo, N Mori, T Yasuda and A Kennedy. Physical modelling of tsunami onshore propagation, peak pressures, and shielding effects in an urban building array. *Coast. Eng.* 2016; **117**, 97-112.

[4] RS Thomas and B Hall. *Seawall design*. Butterworth-Heinemann, London, 1992.

[5] JW Kamphuis. Introduction to coastal engineering and management. *Adv. Ocean Eng.* 2010; **30**, 564.

[6] F Kato, Y Suwa, K Watanabe and S Hatogai. Mechanisms of coastal dike failure induced by the great east japan earthquake tsunami. *Coast. Eng. Proc.* 2012; **1**, 1-9.

[7] SC Hsiao and TC Lin. Tsunami-like solitary waves impinging and overtopping an impermeable seawall: Experiment and RANS modeling. *Coast. Eng.* 2010; **57**, 1-18.

[8] MPR Jayaratne, B Premaratne, A Adewale, T Mikami, S Matsuba, T Shibayama, M Esteban and I Nistor. Failure mechanisms and local scour at coastal structures induced by Tsunami. *Coast. Eng. J.* 2016; **58**, 1-38.

[9] NAK Nandasena, Y Sasaki and N Tanaka. Modeling field observations of the 2011 Great East Japan tsunami: Efficacy of artificial and natural structures on tsunami mitigation. *Coast. Eng.* 2012; **67**, 1-13.

[10] SP Tonkin, M Francis and JD Bricker. Limits on coastal scour depths due to tsunami. *Int. Efforts Lifeline Earthquake Eng.* 2013; **206**, 671-8.

[11] R Maqtan, BY usuf and SB Hamzah. Physical modeling of landward scour due to tsunami bore overtopping seawall. *In*: Proceedings of the International Conference on Civil, Offshore & Environmental Engineering 2018, Kuala Lumpur, Malaysia. 2018, p. 1-11.

[12] T Shimozono and S Sato. Coastal vulnerability analysis during tsunami-induced levee over flow and breaching by a high-resolution flood model. *Coast. Eng.* 2016; **107**, 116-26.

[13] R Jayaratne, A Abimola, T Mikami, S Matsuba, M Esteban and T Shibayama. Predictive model for scour depth of coastal structure failures due to tsunamis. *Coast. Eng. Proc.* 2014; **1**, 1-8.

[14] DR Tappin, HMEvans, CJ Jordan, B Richmond, D Sugawara and K Goto. Coastal changes in the Sendai area from the impact of the 2011 Tohoku-oki tsunami: Interpretations of time series satellite images, helicopter-borne video footage and field observations. *Sediment. Geol.* 2012; **282**, 151-74.

[15] N Tanaka, S Yasuda, K Iimura and J Yagisawa. Combined effects of coastal forest and sea embankment on reducing the washout region of houses in the Great East Japan tsunami. *J. Hydro Environ. Res.* 2014; **8**, 270-80.

[16] N Takegawa, Y Sawada, K Murai and T Kawabata. *Model experiments and simulations on influence of liquefaction on scour at a landward toe of coastal dykes due to tsunami overflow*. University of Southampton, Southampton, England, 2016, p. 1-16.

[17] MS El-Bisy. Bed changes at toe of inclined seawalls. *Ocean Eng.* 2007; **34**, 510-7.

[18] IN Robertson, K Paczkowski, HR Riggs and A Mohamed. Experimental investigation of tsunami bore forces on vertical walls. *J. Offshore Mech. Arctic Eng.* 2013; **135**, 021601.

[19] JD Bricker, M Francis, A Nakayama and G Engineer. Scour depths near coastal structures due to the 2011 Tohoku tsunami. *J. Hydraul. Res.* 2012; **50**, 637-41.

[20] FE Fahlbusch. Scour in rock riverbeds downstream of large dams. *Int. J. Hydropower Dams.* 1994; **1**, 30-2.

[21] P Besley, J Pearson, T Bruce and W Allsop. Wave overtopping at vertical and steep seawalls. *In*: Proceedings of the Institution of Civil Engineers - Maritime Engineering, Auckland, New Zealand. 2005, p. 103-14.

[22] JVD Meer and T Bruce. New physical insights and design formulae on wave overtopping at sloping and vertical structures. *J. Waterway Port Coast. Ocean Eng.* 2014; **140**, 04014025.

[23] JWVD Meer, NWH Allsop, T Bruce, JD Rouck, A Kortenhaus, T Pullen, H Schüttrumpf, P Troch and B Zanuttigh. *Manual on wave overtopping of sea defences and related structures*: *An overtopping manual largely based on European research, but for worldwide application*. German Coastal Engineering Research Council, Hamburg, Germany, 2018.

[24] L Franco, MD Gerloni, JWVD Meer, D Hydraulics, PO Box and AD Emmeloord. Wave overtopping on vertical and composite breakwaters. *Coastal Eng. Proc.* 1994; **1**, 1030-45.
[25] Y Goda. Derivation of unified wave overtopping formulas for seawalls with smooth, impermeable surfaces based on selected CLASH datasets. *Coast. Eng.* 2009; **56**, 385-99.
[26] JVD Meer, W Allsop, T Bruce, JD Rouck, T Pullen, H Schuttrumph, P Troch and B Zanuttigh. Update of the eurotop manual: New insights on wave overtopping. *Coast. Eng. Proc.* 2017; **1**, 1-15.
[27] K Pillai, A Etemad-shahidi and C Lemckert. Wave overtopping at berm breakwaters: Experimental study and development of prediction formula. *Coast. Eng.* 2017; **130**, 85-102.
[28] C Altomare, T Suzuki, X Chen, T Verwaest and A Kortenhaus. Wave overtopping of sea dikes with very shallow foreshores. *Coast. Eng.* 2016; **116**, 236-57.
[29] H Xiao, W Huang and J Tao. Numerical modeling of wave overtopping a levee during hurricane katrina. *Comput. Fluid.* 2008; **38**, 991-6.
[30] A Chadwick, J Morfett and M Borthwick. *Hydraulics in civil and environmental engineering solutions manual.* CRC Press, Florida, 2013, p. 64.
[31] IN Robertson, HR Riggs, K Paczkowski and A Mohamed. Tsunami bore forces on walls. *In*: Proceedings of the ASME 2011 30th International Conference on Ocean, Offshore and Arctic Engineering, Rotterdam, Netherlands. 2011, p. 1-9.
[32] T Rossetto, N Peiris, A Pomonis, S M Wilkinson, R Koo and S Gallocher. The Indian Ocean tsunami of december 26, 2004: Observations in Sri Lanka and Thailand. *Nat. Hazards.* 2007; **42**, 105-24.
[33] HM Fritz, JC Borrero, CE Synolakis and J Yoo. 2004 Indian Ocean tsunami flow velocity measurements from survivor videos. *Geophys. Res. Lett.* 2006; **33**, L24605.
[34] T Rossetto, W Allsop, I Charvet and DI Robinson. Physical modelling of tsunami using a new pneumatic wave generator. *Coast. Eng.* 2011; **58**, 517-27.